American Astronautical Society
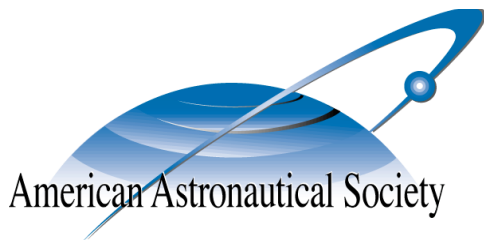
American Institute of
Aeronautics and Astronautics

ANALYTIC SOLUTIONS FOR EQUAL MASS 4-CRAFT STATIC COULOMB FORMATION

Harsh Vasavada and Hanspeter Schaub

AAS/AIAA Astrodynamics Specialist Conference

ANALYTIC SOLUTIONS FOR EQUAL MASS 4-CRAFT STATIC COULOMB FORMATION

Harsh Vasavada[*] and Hanspeter Schaub[†]

This paper investigates analytic constant charge solutions for a square planar and 3-D tetrahedron 4-craft static Coulomb formations. The solutions are formulated in terms of the formation geometry and attitude. In contrast to the 2 and 3 spacecraft Coulomb formations, a 4 spacecraft formation has additional constraints that need to be satisfied for the individual spacecraft charges to be both unique and real. A spacecraft must not only satisfy three inequality 3-craft constraints to yield a real charge solution, but it must also satisfy 2 additional equality constraints to ensure that the spacecraft charges are unique. Further, a method is presented to reduce the number of equality constraints arising due the dynamics of a 4 spacecraft formation. The unique and real spacecraft charges are determined as a function of the orientation of the square formation in a given principal orbit plane. For the 3-D tetrahedron formation scenario there is only a unique set of charged products. The implementability constraints are numerically evaluated to show that only trivial equal-mass tetrahedron formations are possible where one craft is on the along-track axis with zero charge.

INTRODUCTION

Spacecraft formation or general proximity flying is increasingly gaining interest in the aerospace community. The benefits of a spacecraft formation include lower life cycle cost, reconfigurability of the formation shape and size, as well as adaptability of the formation in case of a malfunctioning satellite.[1–4] Applications such as synthetic aperture radar, space interferometry and sensor web formations are more feasible using spacecraft formation flying, rather than large monolithic structures.[1, 2]

For small spacecraft separation distances on the order of 100 meters or less, thruster exhaust plume impingement with neighboring satellites is a major technological hurdle. Further, conventional chemical thrusting concepts are not very effective in generating the small micro-Newton level forces required to maintain a cluster dozens of meters in size. Coulomb thrusting is providing an attractive and a novel solution to these technological hurdles arising from the control of spacecraft in a tight formation.

Geo-stationary spacecraft naturally charge to kilo-volt levels due to their interaction with the local space plasma environment and sun light. For spacecraft flying dozens of meters apart the resulting electrostatic potentials can cause 100's of meters of error motion over an orbit. The concept of Coulomb propulsion varies the spacecraft potential from its natural equilibrium potential using active charge emission. Missions showing the feasibility of active charge control include Equator-S,[5] Geotail,[6, 7] and CLUSTER.[8, 9] With static Coulomb formations constant Coulomb forces are used to cancel out the differential gravitational forces and maintain a fixed formation with respect to the rotating formation chief Local Vertical/Local Horizontal (LVLH) frame. The electrostatic forces acting on the spacecraft are internal forces, and thus cannot change the total inertial angular momentum of the multi-body cluster.

Coulomb thrusting is considered an attractive solution for the control of a tight spacecraft cluster of less than 100 meters in high Earth orbits. While electric propulsion is a very fuel efficient method to control the spacecraft in a formation compared to traditional chemical thrusting concepts, the usefulness of electric propulsion is diminished for small spacecraft separation distances as the ionic exhaust plume could potentially damage near-by spacecraft. Coulomb propulsion has the advantage of being essentially propellant-less and

---
[*]Graduate Student, Aerospace and Ocean Engineering Department, Virginia Tech, Blacksburg, VA, 24061.
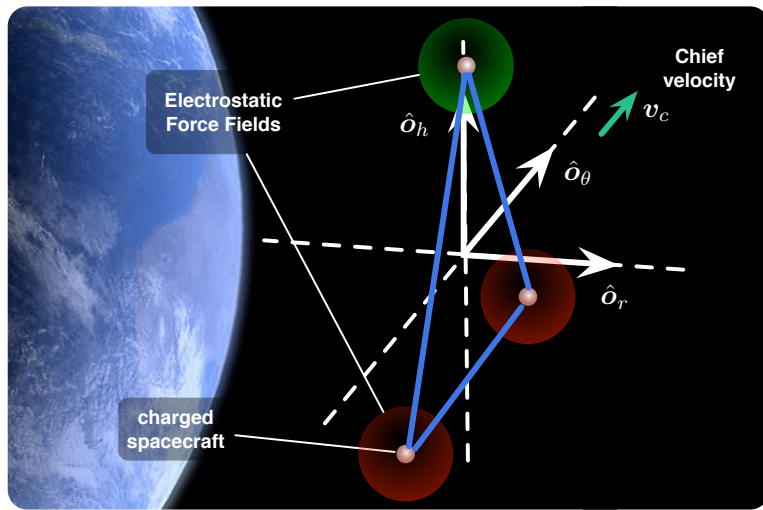[†]Assistant Professor, Virginia Tech, Blacksgurg, VA, 24061-0203

Figure 1 Illustration of a Coulomb virtual structure formation in a circular chief orbit.

offers mass savings up to 98%.[10,11] Coulomb propulsion is a highly efficient propulsion system achieving I_{sp} to the order of 10^{13}s. The power required to charge the spacecraft is in the order of watts (W).[11] In addition to being a highly efficient system, Coulomb propulsion is also based on a renewable source, increasing the mission lifetime as compared to electric propulsion.[12]

Parker and King performed the initial study on Coulomb thrusting in a NASA Institute for Advanced Concepts (NIAC) Phase I project. This NIAC report contains a discussion on Coulomb thrusting, potential applications, and simple techniques to find the static Coulomb formations using symmetry arguments. The report presents analytic solutions for 3 and 5-craft formations and numerical solutions for a 6 spacecraft formation. The report uses simplifying assumptions based on symmetry of the formation to determine the analytic solutions for charges on a spacecraft.

One of the challenging and interesting applications of Coulomb propulsion discussed in the NIAC report is the concept of a static Coulomb formation. The Coulomb forces exactly cancel out the relative motion dynamics creating a virtual Coulomb structure.[12,13] These static solutions are relative equilibrium solutions of the charged relative equations of motion. Berryman and Schaub in Reference 12 extend the work of the NIAC report and present complete analytic solutions for 2 and 3 spacecraft formations.

The necessary equilibrium conditions for static Coulomb formations with constant charges are developed in Reference 14. The conditions require that the center of mass of the static formation structure should be at the origin of the Hill frame. Also, the formation principal inertia axes of the static formation structure need to be aligned with the Hill frame axes. If the center of mass condition is not satisfied the formation drifts relative to the LVLH frame. The principal axes constraints ensure that the gravity gradient torques on the formation are zero.

In a virtual Coulomb structure the truss and beam structural members are replaced with electrostatic force fields. In the presence of external disturbances, the force fields are only able to provide tension and compression to maintain the structural shape of a spacecraft cluster. The force fields maintain this static virtual structure as seen by the rotating Hill frame. Figure 1 shows a Coulomb virtual structure in space. Here the connections between spacecraft represent the electrostatic force fields acting on the spacecraft. The first feedback stabilized 2-craft virtual Coulomb structures are discussed by Natarajan in References 13, 15, 16.

This paper presents analytical open loop charge solutions to establish a 4-craft static Coulomb formation. The charges required are constant and there is no charge feedback to maintain the formation shape. The static formations are naturally occurring equilibrium solutions which are open-loop unstable. How to stabilize the
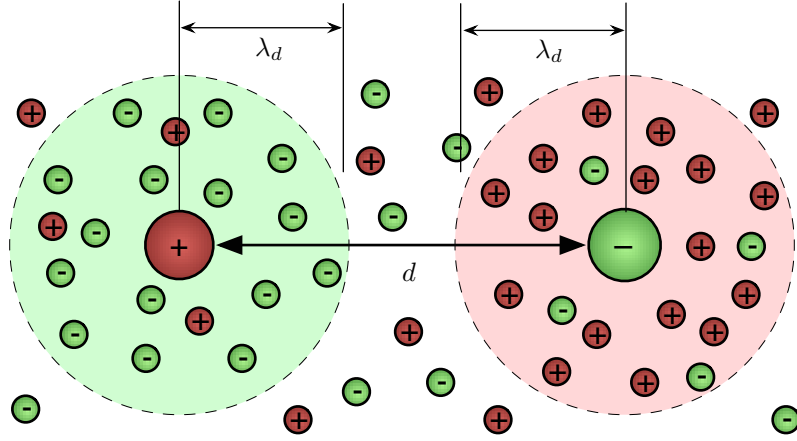
Figure 2 Illustration of Debye shielding in space plasma environment

charged cluster about these equilibrium with 3 or more craft is an open area of research. The analytic solutions presented in this paper extend the work done in References 10 and 12. This paper investigates solutions for particular 4-craft formations, and explores the issue of obtaining unique individual spacecraft charges. This uniqueness issue only appears for formations with 4 or more craft.

Analytic solutions for a square 4-craft formation are discussed first. A square formation is a convenient geometry for missions involving interferometry. All spacecraft are assumed to have equal and constant masses. The second analysis focuses on a 3-D tetrahedron formation. This formation shape is of interest because its symmetry yields zero gravity gradient torque regardless of the formation attitude. The charge implementability conditions are investigated numerically across a range of three-dimensional formation orientations.

COULOMB THRUSTING CONCEPT

The electrostatic Coulomb force between two charged bodies in a vaccum is proportional to the product of the charges and inversely proportional to the square of the distances between them. However, the magnitude of the Coulomb force in a space environment is expressed as

$$F = k_c \frac{q_1 q_2}{d_{ij}^2} e^{-\frac{d_{ij}}{\lambda_d}} \tag{1}$$

Here $k_c = 8.988 \times 10^9$ Nm^{2}C^{-2} is the electrostatic constant and d_{ij} the separation distance between spacecraft. Figure 2 illustrates the interaction between charged bodies in a space evironment. The exponential term in Eq (1) represents the shielding effect of the space plasma environment on the Coulomb force experienced by a second charge body through the term Debye length term λ_d. The plasma field in the space environment reduces the effect of Coulomb interaction by shielding the spacecraft. The Debye length in low Earth orbit is on the order of centimeters, thus requiring spacecraft to be charged to a very large potential to overcome the plasma environment.[10, 11] For the purposes of the analysis in this paper, it is assumed that the spacecraft clusters are in Geostationary Earth Orbits (GEO), where the Debye length ranges from 150m to 1000m, making it more feasible to use Coulomb forces to control the formation. The concept of Coulomb thrusting employs active charge emission devices to expel electrons or ions to modify the natural electrostatic equilibrium of the spacecraft.

Coulomb propulsion has potential uses in spacecraft cluster applications other than static Coulomb formations. Natarajan and Schaub present the 2-craft Coulomb tether structure concept in Reference 13. Here an electrostatic field replaces the physical tether. The paper also presents the use of the gravity-gradient torque to stabilize the virtual Coulomb structure about the orbit nadir direction. Reference 13 also presents the
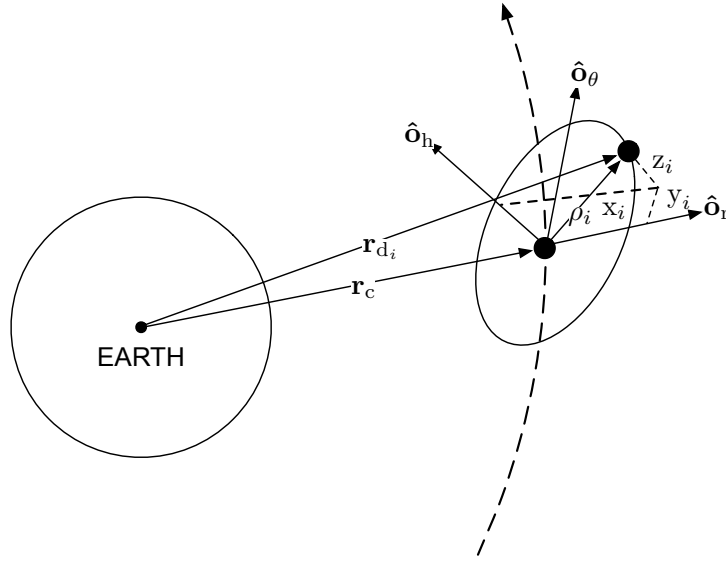
Figure 3   Illustration of Hill Frame Coordinate system

first feedback law for a stabilized virtual Coulomb structure, with the separation distance and time rate of separation distance as the feedback terms.

References 17 and 18 develop control laws to maintain a charged spacecraft cluster. Reference 17 develops a non-linear control law based on orbit element differences to control a 2-craft Coulomb formation. The paper also proves the stability of such a control law. Reference 18 discusses the potential use of electrostatic Coulomb forces for spacecraft collision avoidance using separation distance as feedback.

Another exciting application of Coulomb propulsion is given by Pettazzi et.al in Reference 19. Here the hybrid use of electrostatic forces and conventional thrusting for swarm navigation and reconfiguration is discussed. The paper also discusses the different strategies for integrating the Coulomb actuation into swarm navigation and reconfiguration scheme. Application of Coulomb forces in aiding the self-assembly of the large space structures is discussed in Reference 20.

CHARGED SPACECRAFT EQUATIONS OF MOTION

Let us define the rotating Hill coordinate system $\mathcal{H}$ with respect to which the relative motion dynamics of the spacecraft formation is expressed. The Hill frame is defined as $\mathcal{H} = \{O, \hat{\mathbf{o}}_r, \hat{\mathbf{o}}_\theta, \hat{\mathbf{o}}_h\}$ as illustrated in figure 3. Here the origin of the Hill frame lies at the center of mass of the formation. The vector $\hat{\mathbf{o}}_r$ points radially outward, $\hat{\mathbf{o}}_h$ points in the out of plane direction, and the along-track direction $\hat{\mathbf{o}}_\theta$ completes the coordinate system such that $\hat{\mathbf{o}}_\theta = \hat{\mathbf{o}}_h \times \hat{\mathbf{o}}_r$. The relative position vector between the deputy and the chief in interial frame is expressed as $\boldsymbol{\rho_i} = \mathbf{r}_{d_i} - \mathbf{r}_c$, where $\mathbf{r}_{d_i}$ is the inertial position of the deputy spacecraft and $\mathbf{r}_c$ is the inertial position of the chief satellite. The relative position vector in Hill frame component is expressed as

$$\boldsymbol{\rho}_i = {}^{\mathcal{H}}\begin{pmatrix} x_i \\ y_i \\ z_i \end{pmatrix} \tag{2}$$

The conditions for a static Coulomb formation are achieved by allowing the electrostatic forces to cancel out the relative acceleration experienced in the Hill frame. Using the definition of electrostatic force given in

4

equation (1), the charged relative equations of motion with linearized orbital motion are written as[12]

$$\ddot{x}_i - 2n\dot{y}_i - 3n^2 x_i \quad = \quad \sum_{j=1}^{N} \frac{k_c}{m_i} \frac{x_i - x_j}{d_{ij}^3} q_i q_j e^{-\frac{d_{ij}}{\lambda_d}} \tag{3a}$$

$$\ddot{y}_i + 2n\dot{x}_i \quad = \quad \sum_{j=1}^{N} \frac{k_c}{m_i} \frac{y_i - y_j}{d_{ij}^3} q_i q_j e^{-\frac{d_{ij}}{\lambda_d}} \tag{3b}$$

$$\ddot{z}_i + n^2 z_i \quad = \quad \sum_{j=1}^{N} \frac{k_c}{m_i} \frac{z_i - z_j}{d_{ij}^3} q_i q_j e^{-\frac{d_{ij}}{\lambda_d}} \tag{3c}$$

Here subscript i indicates the ith position in the spacecraft formation, d_{ij} is the distance between the ith and j^{th} spacecraft, and n is the mean orbit rate.

To find a charged relative equilibrium, the relative acceleration and velocity of the spacecraft are set to zero, freezing the formation with respect to the Hill frame. The individual spacecraft charges q_i can be scaled through:

$$\tilde{q}_i = \frac{\sqrt{k_c}}{n} q_i \tag{4}$$

The normalized spacecraft charge $\tilde{q}_i$, is not a non-dimensional charge. Using Eq. (4) and the definition of charged product as $Q_{ij} = \tilde{q}_i \tilde{q}_j$, the charged spacecraft equations of motion are written as[12]

$$-3x_i = \sum_{i=1}^{N} \frac{1}{m_i} \frac{x_i - x_j}{d_{ij}^3} \tilde{Q}_{ij} \tag{5a}$$

$$0 = \sum_{i=1}^{N} \frac{1}{m_i} \frac{y_i - y_j}{d_{ij}^3} \tilde{Q}_{ij} \tag{5b}$$

$$z_i = \sum_{i=1}^{N} \frac{1}{m_i} \frac{z_i - z_j}{d_{ij}^3} \tilde{Q}_{ij} \tag{5c}$$

Note that for a formation in which the spacecraft are aligned with the along-track ($\hat{\mathbf{o}}_\theta$) direction, there are no spacecraft charges required to achieve the relative equilibrium.

4-CRAFT STATIC COULOMB PLANAR FORMATION SOLUTIONS

A square planar formation lies in the principal planes defined by $\hat{\mathbf{o}}_r$-$\hat{\mathbf{o}}_h$, $\hat{\mathbf{o}}_r$-$\hat{\mathbf{o}}_\theta$ or $\hat{\mathbf{o}}_h$-$\hat{\mathbf{o}}_\theta$ planes. The formation lies entirely in these planes and there is no out of plane component. A square formation is one of the possible 4-craft planar formations. The square formation geometry is convenient for interferometric missions where the craft are ideal distributed on a projected circle orthogonal to the sensing axis. The center of mass condition is satisfied by placing the center of the square at the origin of the Hill frame. The square is rotated in the principal plane about the third axis. Note that the principal axes constraint is satisfied for any square orientation within the principal orbit plane.

Charge Products for Relative Equillibrium

A planar square formation can be parameterized in terms of the angle θ and the radius ρ as illustrated in figure 4. The angle θ represents the orientation of the square formation in any given plane. The radius ρ is the distance of the spacecraft from the origin of the Hill frame. Figure 4 shows the square formation in $\hat{\mathbf{o}}_r$-$\hat{\mathbf{o}}_\theta$ plane, where the square is rotated through an angle of $\theta = 45°$ from its nominal position of $\theta = 0°$. The square can be parametrized in a similar manner for $\hat{\mathbf{o}}_h$-$\hat{\mathbf{o}}_\theta$ and $\hat{\mathbf{o}}_r$-$\hat{\mathbf{o}}_h$ plane. For the formation in the $\hat{\mathbf{o}}_r$-$\hat{\mathbf{o}}_\theta$ plane, the position vectors of the 4 spacecraft are given by
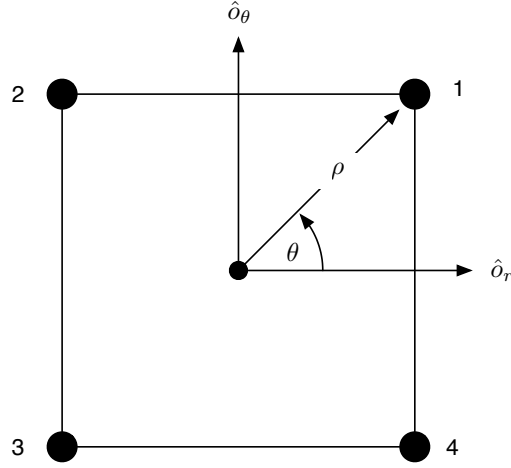
Figure 4 Planar 4-Satellite formation in $\hat{o}_r - \hat{o}_h$ plane

$$\boldsymbol{\rho}_1 = \begin{pmatrix} \rho\cos\theta \\ \rho\sin\theta \\ 0 \end{pmatrix}, \ \boldsymbol{\rho}_2 = \begin{pmatrix} -\rho\sin\theta \\ \rho\cos\theta \\ 0 \end{pmatrix}, \ \boldsymbol{\rho}_3 = \begin{pmatrix} -\rho\cos\theta \\ -\rho\sin\theta \\ 0 \end{pmatrix}, \ \boldsymbol{\rho}_4 = \begin{pmatrix} \rho\sin\theta \\ -\rho\cos\theta \\ 0 \end{pmatrix}$$

With a square formation there are 8 non-trivial charged equations of motion from Eq. (5), 4 each in the $\hat{\mathbf{o}}_r$ and $\hat{\mathbf{o}}_\theta$ directions. The number of these equations is reduced by applying the center of mass conditions and principal axes constraints.[14] These conditions require that the center of mass of the static formation lie at the origin of the Hill frame, and the principal axes of the static formation be aligned with the axes of the rotating Hill frame. Due to symmetry for a planar formation there are 2 center of mass constraints and 1 principal axes constraint. The number of equations is now reduced to 5. Thus applying the center of mass and principal axes constraint and using Eqs. (5a)$-$(5c), the formation dynamics in $\hat{o}_r - \hat{o}_\theta$ is expressed in matrix form as

$$\begin{bmatrix} -3mx_1 \\ -3mx_2 \\ -3mx_3 \\ 0 \\ 0 \end{bmatrix} = \begin{bmatrix} \frac{x_1-x_2}{d_{12}^3} & \frac{x_1-x_3}{d_{13}^3} & \frac{x_1-x_4}{d_{14}^3} & 0 & 0 & 0 \\ \frac{x_2-x_1}{d_{12}^3} & 0 & 0 & \frac{x_2-x_3}{d_{23}^3} & \frac{x_2-x_4}{d_{24}^3} & 0 \\ 0 & \frac{x_3-x_1}{d_{13}^3} & 0 & \frac{x_3-x_2}{d_{23}^3} & 0 & \frac{x_3-x_4}{d_{34}^3} \\ \frac{y_1-y_2}{d_{12}^3} & \frac{y_1-y_3}{d_{13}^3} & \frac{y_1-y_4}{d_{14}^3} & 0 & 0 & 0 \\ \frac{y_2-y_1}{d_{12}^3} & 0 & 0 & \frac{y_2-y_3}{d_{23}^3} & \frac{y_2-y_4}{d_{24}^3} & 0 \end{bmatrix} \begin{bmatrix} \tilde{Q}_{12} \\ \tilde{Q}_{13} \\ \tilde{Q}_{14} \\ \tilde{Q}_{23} \\ \tilde{Q}_{24} \\ \tilde{Q}_{34} \end{bmatrix} \tag{6}$$

where $d_{ij} = \sqrt{(x_i - x_j)^2 + (y_i - y_j)^2}$ is the distance between the ith and j^{th} spacecraft. Equation (6) is expressed in compact form as

$$\mathbf{x} = [A]\tilde{\mathbf{Q}} \tag{7}$$

The matrix $[A]$ only depends upon the orientation angle θ and the radius ρ of the spacecraft. It is interesting to note that $[A]$ does not depend on the plane in which the formation is oriented. The null-space of $[A]$ is identical for any given plane. To solve for the individual charges on spacecraft, a solution to the charged products $\tilde{Q}_{ij}$ is required. The rank of matrix $[A]$ is 5, and it is a full row rank matrix. There are infinitely many solutions to $\tilde{\mathbf{Q}}$, which can be expressed in terms of least squares solution, $\mathbf{Q}^*$, and the null-space $\mathbf{Q}_{\text{null}}$. The least squares solution for the system described by (7) is given by

$$\mathbf{Q}^* = [A]^T \left([A][A]^T\right)^{-1} \mathbf{x} \tag{8}$$
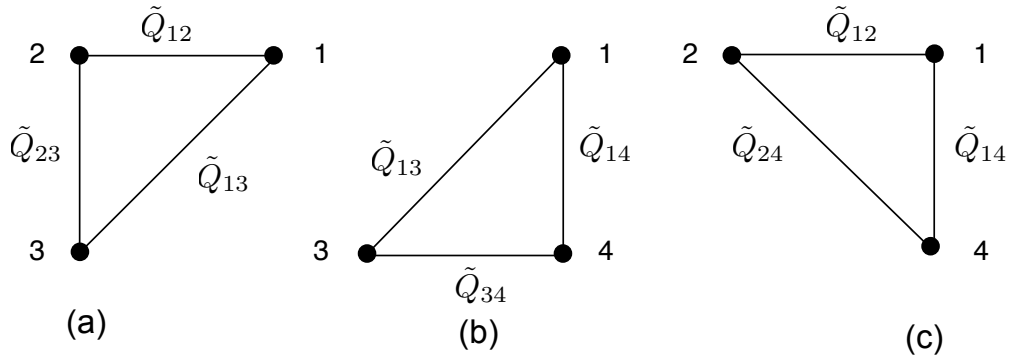
6

Figure 5   Breakdown of a square formation into triangular loops

All the possible solutions for $\tilde{\mathbf{Q}}$ are

$$\tilde{\mathbf{Q}} = \mathbf{Q}^* + t\mathbf{Q}_{null} \tag{9}$$

where t is a scalar used to scale the null space of $[A]$. For the given $\hat{\mathbf{o}}_r$-$\hat{\mathbf{o}}_\theta$ plane, the least squares solution and the null space of the system are

$$\mathbf{Q}^* = \begin{bmatrix} -\frac{3\sqrt{2}}{10} m\rho^3 \left(4 + 5\sin 2\theta\right) \\ -\frac{6}{5} m\rho^3 \left(1 + 5\cos 2\theta\right) \\ \frac{3\sqrt{2}}{10} m\rho^3 \left(-4 + 5\sin 2\theta\right) \\ \frac{3\sqrt{2}}{10} m\rho^3 \left(-4 + 5\sin 2\theta\right) \\ -\frac{6}{5} m\rho^3 \left(1 - 5\cos 2\theta\right) \\ -\frac{3\sqrt{2}}{10} m\rho^3 \left(4 + 5\sin 2\theta\right) \end{bmatrix} \tag{10}$$

$$\mathbf{Q}_{null} = \begin{bmatrix} 1 & -2\sqrt{2} & 1 & 1 & -2\sqrt{2} & 1 \end{bmatrix}^T \tag{11}$$

The least squares solution, for the $\hat{\mathbf{o}}_r$-$\hat{\mathbf{o}}_\theta$ plane depends on the size of the square formation and the orientation of the square in the plane. The null-space of the system does not depend on the orientation of the formation, and as discussed earlier is the same for any given plane.

Unique Spacecraft Charges

To implement a static Coulomb formation, knowledge of the individual charges on a spacecraft is required. For a 4-craft formation there are 6 charge products, which results in 4 individual spacecraft charges. This is always true for a 4-craft formation, regardless of whether the formation is co-linear, planar or three-dimensional. There are infinitely many ways to solve for the individual charges from the charge products. To solve for $\tilde{q}_1$, we can break up the square into 3 different triangular loops about the spacecraft position 1 as shown in figure 5. From the loops defined in figure 5, $\tilde{q}_1$ can be calculated either of Eqs. (12a)–(12c):

$$\tilde{q}_{1a} = \sqrt{\frac{\tilde{Q}_{12}\tilde{Q}_{13}}{\tilde{Q}_{23}}} \tag{12a}$$

$$\tilde{q}_{1b} = \sqrt{\frac{\tilde{Q}_{12}\tilde{Q}_{14}}{\tilde{Q}_{24}}} \tag{12b}$$

7

$$\tilde{q}_{1c} = \sqrt{\frac{\tilde{Q}_{14}\tilde{Q}_{13}}{\tilde{Q}_{34}}} \tag{12c}$$

For the individual charges on a spacecraft to be unique Eqs. (12a)-(12c) must yield the exact same value of $\tilde{q}_1$, which mathematically is written as the equality constraints

$$\tilde{q}_1 = \sqrt{\frac{\tilde{Q}_{12}\tilde{Q}_{13}}{\tilde{Q}_{23}}} = \sqrt{\frac{\tilde{Q}_{12}\tilde{Q}_{14}}{\tilde{Q}_{24}}} = \sqrt{\frac{\tilde{Q}_{14}\tilde{Q}_{13}}{\tilde{Q}_{34}}} \tag{13}$$

The charged products in the above equation depend on the scaling parameter t in Eq. (9). Given a unique $\tilde{q}_1$, the remaining individual charges are trivially calculated as

$$\tilde{q}_2 = \frac{\tilde{Q}_{12}}{\tilde{q}_1} \tag{14a}$$

$$\tilde{q}_3 = \frac{\tilde{Q}_{13}}{\tilde{q}_1} \tag{14b}$$

$$\tilde{q}_4 = \frac{\tilde{Q}_{14}}{\tilde{q}_1} \tag{14c}$$

In a 3 spacecraft formation there is only one triangular loop and it results in a unique individual charge. However, in a 4-craft formation there are two additional triangular loops. These make the task of determining the individual spacecraft charges non-trivial. First, assume that $\tilde{q}_{1a}$ and $\tilde{q}_{1b}$ from Eqs. (12a) and (12b) are equal.

$$\sqrt{\frac{\tilde{Q}_{12}\tilde{Q}_{13}}{\tilde{Q}_{23}}} = \sqrt{\frac{\tilde{Q}_{14}\tilde{Q}_{13}}{\tilde{Q}_{34}}} \tag{15}$$

Assuming $\tilde{Q}_{13} \neq 0$ which would yield a trivial non-charged solution, Eq. (15) is simplified to

$$\tilde{Q}_{12}\tilde{Q}_{34} - \tilde{Q}_{14}\tilde{Q}_{23} = 0 \tag{16}$$

Using Eqs. (9)-(11), Eq. (16) is written as

$$\left(-\frac{3\sqrt{2}}{10}m\rho^3\left(4 + 5\sin 2\theta\right) + t\right)^2 - \left(-\frac{3\sqrt{2}}{10}m\rho^3\left(4 - 5\sin 2\theta\right) + t\right)^2 = 0 \tag{17}$$

Simplifying further yields

$$\frac{6}{5}m\rho^3\left(-5\sqrt{2}t + 12m\rho^3\right)\sin\left(2\theta\right) = 0 \tag{18}$$

Thus the quadratic equation in (17) simplifies to a linear equation with one root, which can be solved for t where the individual charges are unique. Equation (18) is also true when $\sin 2\theta = 0$. Thus unique charges can be found for specific orientation angles of $\theta = 0°$ and $\theta = 90°$. Such an orientation corresponds to two spacecraft aligned along the $\hat{\mathbf{o}}_\theta$ axes and the remaining 2 spacecraft aligned along the $\hat{\mathbf{o}}_r$ axes. Solving Eq. (18), the value of t for which Eq. (15) holds true is

$$t = \frac{6\sqrt{2}}{5}m\rho^3 \tag{19}$$

The value of scalar t in Eq. (19) ensures that a unique $\tilde{q}_1$ is found from the equality constraint in Eq (16). To prove that the second equality constraint is satisfied, let us explore the third uniqueness condition in Eq. (12c). Eq. (12c) can also be written as

$$\tilde{q}_{1c} = \sqrt{\frac{\tilde{Q}_{14}\tilde{Q}_{12}}{\tilde{Q}_{24}} \cdot \frac{\tilde{Q}_{13}\tilde{Q}_{24}}{\tilde{Q}_{34}\tilde{Q}_{12}}} = \sqrt{\tilde{q}_{1b}^2 \cdot \frac{\tilde{Q}_{13}\tilde{Q}_{24}}{\tilde{Q}_{34}\tilde{Q}_{12}}} \tag{20}$$

Thus it is seen that Eq. (12c) is same as (12b) if

$$\frac{\tilde{Q}_{13}\tilde{Q}_{24}}{\tilde{Q}_{34}\tilde{Q}_{12}} = 1 \tag{21}$$

Using the value of scaling parameter t from (19) and Eqs. (10) and (11), Eq. (9) is rewritten as

$$\tilde{\mathbf{Q}} = m\rho^3 \begin{bmatrix} -3\sqrt{2}\cos\theta\sin\theta \\ -3\sqrt{2}\cos^2\theta \\ 3\sqrt{2}\cos\theta\sin\theta \\ 3\sqrt{2}\cos\theta\sin\theta \\ -3\sqrt{2}\sin^2\theta \\ -3\sqrt{2}\cos\theta\sin\theta \end{bmatrix} \tag{22}$$

Using the values of $\tilde{Q}_{ij}$ in Eq. (22), Eq. (21) is rewritten as

$$\frac{\tilde{Q}_{13}\tilde{Q}_{24}}{\tilde{Q}_{34}\tilde{Q}_{12}} = \frac{\left(-3\sqrt{2}\sin^2\theta\right)\left(-3\sqrt{2}\cos^2\theta\right)}{\left(-3\sqrt{2}\sin\theta\cos\theta\right)\left(-3\sqrt{2}\sin\theta\cos\theta\right)} = 1 \tag{23}$$

Thus the condition in Eq. (12c) is satisfied and that Eq. (12c) will yield the same $\tilde{q}_1$ as Eq. (12b). It is shown that to obtain a unique spacecraft charge only one equality constraints from Eqs. (12a) - (12c) needs to be satisfied, as the second one is guaranteed to be true. This argument is only true for a square planar formation with equal spacecraft masses.

Carefully choosing the value of the null-space scaling parameter t, the number of equality constraints for unique spacecraft charges are reduced to 1. This method does not take into consideration that unique spacecraft charges exist for specific orientation angles of $\theta = 0°$ and $\theta = 90°$. For $\theta = 0°$, the charged products solutions is

$$\tilde{\mathbf{Q}} = \begin{bmatrix} t - \frac{6}{5}\sqrt{2}m\rho^3 \\ -2\sqrt{2}t - \frac{36}{5}m\rho^3 \\ t - \frac{6}{5}\sqrt{2}m\rho^3 \\ t - \frac{6}{5}\sqrt{2}m\rho^3 \\ -2\sqrt{2}t + \frac{24}{5}m\rho^3 \\ t - \frac{6}{5}\sqrt{2}m\rho^3 \end{bmatrix} \tag{24}$$

It is seen from equation (24,) that only 1 equality constraint needs to be satisfied for unique spacecraft charges as $\tilde{Q}_{12}\tilde{Q}_{34} = \tilde{Q}_{14}\tilde{Q}_{23}$. The null-space scaling parameter t can be chosen in a manner such that equation (21) is satisfied. Using the values of charged production in Eq. (24), Eq. (21) is rewritten as

$$7t^2 - \frac{36}{5}\sqrt{2}m\rho^3 t + \frac{936}{5}m^2\rho^6 = 0 \tag{25}$$

Equation (25) is a quadratic equation. There are two possible values of null-space scaling parameter t where unique charges can be found for orientation angle $\theta = 0°$. Solving Eq. (25) the values of t for which unique spacecraft charges exist are

$$t_1 = \frac{6}{5}\sqrt{2}m\rho^3 \tag{26a}$$

$$t_2 = -\frac{78}{35}\sqrt{2}m\rho^3 \tag{26b}$$

From Eq. (26a) it is noted that the value of null-space scaling parameter t is same as in equation (19). This implies that it is possible for find real spacecraft charges for orientations other than $\theta = 0°$ or $\theta = 90°$. However if the null-space scaling parameter is used from Eq. (26b), then real charges can only be found for

9

$\theta = 0°$ or $\theta = 90°$. The steps in Eqs. (24) to (26) are for $\theta = 90°$. For $\theta = 90°$, the null-space scaling parameter for unique charges is the same as in Eq. (26).

Without loss of generality, the steps from Eqs. (12) to (26) can be repeated for the other two planes $\hat{\mathbf{o}}_h$-$\hat{\mathbf{o}}_\theta$ and $\hat{\mathbf{o}}_r$-$\hat{\mathbf{o}}_h$. The formation dynamics in $\hat{\mathbf{o}}_h$-$\hat{\mathbf{o}}_\theta$ is written as

$$m \begin{bmatrix} -3z_1 \\ -3z_2 \\ -3z_3 \\ 0 \\ 0 \end{bmatrix} = \begin{bmatrix} \frac{\cos\theta+\sin\theta}{2\sqrt{2}\rho^2} & \frac{\cos\theta}{4\rho^2} & \frac{\cos\theta-\sin\theta}{2\sqrt{2}\rho^2} & 0 & 0 & 0 \\ \frac{-\cos\theta+\sin\theta}{2\sqrt{2}\rho^2} & 0 & 0 & \frac{\cos\theta-\sin\theta}{2\sqrt{2}\rho^2} & -\frac{\sin\theta}{4\rho^2} & 0 \\ 0 & -\frac{\cos\theta}{4\rho^2} & 0 & \frac{-\cos\theta+\sin\theta}{2\sqrt{2}\rho^2} & 0 & \frac{\cos\theta+\sin\theta}{2\sqrt{2}\rho^2} \\ \frac{-\cos\theta+\sin\theta}{2\sqrt{2}\rho^2} & \frac{\sin\theta}{4\rho^2} & \frac{\cos\theta+\sin\theta}{2\sqrt{2}\rho^2} & 0 & 0 & 0 \\ \frac{\cos\theta-\sin\theta}{2\sqrt{2}\rho^2} & 0 & 0 & \frac{\cos\theta+\sin\theta}{2\sqrt{2}\rho^2} & \frac{\cos\theta}{4\rho^2} & 0 \end{bmatrix} \begin{bmatrix} \tilde{Q}_{12} \\ \tilde{Q}_{13} \\ \tilde{Q}_{14} \\ \tilde{Q}_{23} \\ \tilde{Q}_{24} \\ \tilde{Q}_{34} \end{bmatrix}$$

(27)

Equation (16) for $\hat{\mathbf{o}}_h$-$\hat{\mathbf{o}}_\theta$ plane is written as

$$-\frac{2}{5}m\rho^3 \left(5\sqrt{2}t + 4m\rho^3\right)\sin 2\theta = 0 \tag{28}$$

The value of t for which the unique spacecraft charges is:

$$t = \frac{-4}{5\sqrt{2}}m\rho^3 \tag{29}$$

Unique spacecraft charges can also be computed for $\theta = 0°$ or $\theta = 90°$. The null-space scaling factor t required for unique spacecraft charges is

$$t_1 = -\frac{4}{5\sqrt{2}}m\rho^3 \tag{30a}$$

$$t_2 = \frac{52}{35\sqrt{2}}m\rho^3 \tag{30b}$$

It is noted that the value of null-space scaling factor in Eq. (30a) is the same as in Eq. (29). Thus real charges can be computed for any orientation of square in the $\hat{\mathbf{o}}_h$-$\hat{\mathbf{o}}_\theta$ plane. However if the value of scaling parameter from Eq. (30a) is used, real charges can only be computed for $\theta = 0°$ or $\theta = 90°$.

The formation dynamics in the $\hat{\mathbf{o}}_r$-$\hat{\mathbf{o}}_h$ plane is written as

$$m \begin{bmatrix} -3x_1 \\ -3x_2 \\ -3x_3 \\ z_1 \\ z_2 \end{bmatrix} = \begin{bmatrix} \frac{\cos\theta+\sin\theta}{2\sqrt{2}\rho^2} & \frac{\cos\theta}{4\rho^2} & \frac{\cos\theta-\sin\theta}{2\sqrt{2}\rho^2} & 0 & 0 & 0 \\ \frac{-\cos\theta+\sin\theta}{2\sqrt{2}\rho^2} & 0 & 0 & \frac{\cos\theta-\sin\theta}{2\sqrt{2}\rho^2} & -\frac{\sin\theta}{4\rho^2} & 0 \\ 0 & -\frac{\cos\theta}{4\rho^2} & 0 & \frac{-\cos\theta+\sin\theta}{2\sqrt{2}\rho^2} & 0 & \frac{\cos\theta+\sin\theta}{2\sqrt{2}\rho^2} \\ \frac{-\cos\theta+\sin\theta}{2\sqrt{2}\rho^2} & \frac{\sin\theta}{4\rho^2} & \frac{\cos\theta+\sin\theta}{2\sqrt{2}\rho^2} & 0 & 0 & 0 \\ \frac{\cos\theta-\sin\theta}{2\sqrt{2}\rho^2} & 0 & 0 & \frac{\cos\theta+\sin\theta}{2\sqrt{2}\rho^2} & \frac{\cos\theta}{4\rho^2} & 0 \end{bmatrix} \begin{bmatrix} \tilde{Q}_{12} \\ \tilde{Q}_{13} \\ \tilde{Q}_{14} \\ \tilde{Q}_{23} \\ \tilde{Q}_{24} \\ \tilde{Q}_{34} \end{bmatrix}$$

(31)

Equation (16) for $\hat{\mathbf{o}}_h$-$\hat{\mathbf{o}}_\theta$ plane is written as

$$-\frac{2}{5}m\rho^3 \left(5\sqrt{2}t + 4m\rho^3\right)\sin 2\theta = 0 \tag{32}$$

The value of t for which the unique spacecraft charges can be found is.

$$t = \frac{4}{5}\sqrt{2}m\rho^3 \tag{33}$$

10

Unique spacecraft charges can also be computed for $\theta = 0°$ or $\theta = 90°$. The null-space scaling factor t required for unique spacecraft charges is

$$t_1 = -\frac{4}{35}m\rho^3\left(3\sqrt{2} - 5\sqrt{29}\right) \tag{34a}$$

$$t_2 = -\frac{4}{35}m\rho^3\left(3\sqrt{2} + 5\sqrt{29}\right) \tag{34b}$$

It is noted that unlike $\hat{\mathbf{o}}_r$-$\hat{\mathbf{o}}_\theta$ and $\hat{\mathbf{o}}_h$-$\hat{\mathbf{o}}_\theta$ planes the value of null-space scaling factor in Eq. (34) is not common to the scaling parameter for arbitrary orientations. Real charges can be computed for any orientation of square in the $\hat{\mathbf{o}}_r$-$\hat{\mathbf{o}}_h$ plane using the scaling parameter in equation (33). If the value of scaling parameter from Eq. (34b) or (34a) is used, real charges can only be computed for $\theta = 0\circ$ or $\theta = 90°$.

From Eqs. (19),(29) and (33), it is evident that for an arbitrary orientation of a formation in the given plane, only one set of unique individual charges on the spacecraft exists. Further the value of the scalar t where these unique charges exist is a constant in a given plane and does not depend on the orientation θ of the formation within the given plane. However it is also possible to find unique spacecraft charges for specific orientations of $\theta = 0°$ or $\theta = 90°$.

Real Charges

Finding unique spacecraft charges is not a sufficient condition for the formation to exist; the charges on the spacecraft in a formation also need to be real. In a 3-craft formation, there is only one inequality constraint for real charges. For a 4-craft formation, there are two additional constraints. Mathematically the conditions for real charges are expressed as the inequality constraints

$$\tilde{Q}_{12} \cdot \tilde{Q}_{13} \cdot \tilde{Q}_{23} > 0 \tag{35a}$$

$$\tilde{Q}_{12} \cdot \tilde{Q}_{14} \cdot \tilde{Q}_{24} > 0 \tag{35b}$$

$$\tilde{Q}_{13} \cdot \tilde{Q}_{14} \cdot \tilde{Q}_{34} > 0 \tag{35c}$$

For real spacecraft charges in a 3-craft formation the inequality constraint in Eq. (35a) needs to be true. The additional constraints for real spacecraft in Eqs. (35b) and (35c) need to be satisfied for a 4-craft formation. Using Eq. (12a) Eq. (35a) can be written as

$$\tilde{q}_1^2 \cdot \left(\tilde{Q}_{23}\right)^2 > 0 \tag{36}$$

Assuming the real charge condition in Eq. (35a) is satisfied. We find $\tilde{q}_1^2 > 0$ as $\tilde{Q}_{23}^2 > 0$ for all values of $\tilde{Q}_{23}$. Similarly equations (35b) and (35c) are expressed as

$$\tilde{q}_1^2 \cdot \left(\tilde{Q}_{24}\right)^2 > 0 \tag{37}$$

$$\tilde{q}_1^2 \cdot \left(\tilde{Q}_{34}\right)^2 > 0 \tag{38}$$

Because it was already proven that $q_1^2 > 0$ as Eq. (35a) is true; the other two inequality constraints (35b) and (35c) are guaranteed to be satisfied. While the individual charge $\tilde{q}_1$ is the unique spacecraft charge required on a formation, the arguments in equations (35a)-(35c) are valid for any 4-craft formation, not just the special case of the square formation being considered here.

Using the null-space of $\tilde{\mathbf{Q}}$ in (9) Eq. (35a) is expanded as a cubic polynomial in terms of the scalar t. The roots of this polynomial expressed in terms of θ and ρ are

$$\begin{array}{l} t_1 = -\frac{3}{5\sqrt{2}}m\rho^3\left(1 + 5\cos 2\theta\right) \\ t_2 = \frac{3}{5\sqrt{2}}m\rho^3\left(2 - 5\sin 2\theta\right) \\ t_3 = \frac{3}{5\sqrt{2}}m\rho^3\left(2 + 5\sin 2\theta\right) \end{array} \tag{39}$$

(a) Valid regions for charges to be real for $\theta = 30°$ (b) Range of θ for real charges for $\hat{o}_r - \hat{o}_\theta$ plane

Figure 6 Plot of regions where unique spacecraft charges are real

The range of t for which the inequality constraint (35a) is satisfied, can be determined in terms of the roots in Eq. (39). Wang in Reference 21 exploits the 1-D null-space to parametrize the inequality constraint for real charges. For the 1-D constrained 3-craft he presents an elegant method for determining the regions of real charges in terms of the roots in Eq. (35a). Let $\hat{a}$, $\hat{b}$ and $\hat{c}$ represent Q_{12}^*, Q_{13}^* and Q_{23}^* respectively from (10), using this parametrization and (11), Eq.(35a) can be written down as

$$f(t) = (\hat{a} + t)\left(\hat{b} - 2\sqrt{2}t\right)(\hat{c} + t) > 0 \tag{40}$$

Let a, b and c be the roots of the polynomial in Eq. (40), arranged in the following order $a > b > c$. An interesting property of the polynomial in Eq. (40) is as $\lim_{t\to\infty} f(t) < 0$ and $\lim_{t\to-\infty} f(t) > 0$. Thus the inequality constraint in (35a) is satisfied in the region b $< t <$ a and $t <$ c.

Figure 6(a) shows the shape of the general polynomial described by equation (40) and the valid regions of t where $f(t) > 0$. Figure 6(b) plots $\tilde{t}_i$ for $0° \leq \theta \leq 90°$, where $\tilde{t}_i = \frac{5\sqrt{2}}{3m\rho^3}t_i$. The shaded regions show the range of θ where the individual charges are real. Figure 6(b) also plots the value of null-space scaling factor for unique charges in equation (26). For a solution to exist, the value of t in (26) and should lie in the shaded region of the plot in figure 6(b). From the figure we can see for the individual charges to be real and implementable, the square can be rotated between $0 \leq \theta \leq 90$ degrees from $\hat{o}_r$ axis for the formation to be possible. Table 1 shows the order of roots arranged in terms of the orientation of the square in the $\hat{o}_r$-$\hat{o}_\theta$ plane.

θ	Order of Roots
$0 < \theta < 45$	$t_2 > t_3 > t_1$
$45 < \theta < 90$	$t_2 > t_1 > t_3$

Table 1 Order of Roots depending on angle of orientation for $\hat{o}_r - \hat{o}_\theta$ plane

The individual charges now can be calculated by substituting in the value of t from (19) in equation (12a)

Figure 7   Plot of θ for real and unique charges.

to get q_1 in terms of ρ and θ.

$$\tilde{q}_1 = \sqrt{3\sqrt{2}m\rho^3}\cos\theta \tag{41a}$$

$$\tilde{q}_2 = \sqrt{3\sqrt{2}m\rho^3}\sin\theta \tag{41b}$$

$$\tilde{q}_3 = -\sqrt{3\sqrt{2}m\rho^3}\cos\theta \tag{41c}$$

$$\tilde{q}_4 = -\sqrt{3\sqrt{2}m\rho^3}\sin\theta \tag{41d}$$

The individual charges found in Eq. (41) are only valid for $t = \frac{6}{5}\sqrt{2}m\rho^3$. From figure 6(b) it can be seen that for $\theta = 0°$ or $\theta = 90°$ and $t = \frac{6}{5}\sqrt{2}m\rho^3$ unique and real spacecraft charges exist. While $\theta = 0°$ spacecraft 2 and 4 are aligned along $\hat{\mathbf{o}}_\theta$ axis and have no charges acting on them. It is also noted when $t = \frac{6}{5}\sqrt{2}m\rho^3$ unique and real charges exist for formation orientations other than $\theta = 0°$ or $\theta = 90°$. It is also observed that when $t = -\frac{78}{35}\sqrt{2}m\rho^3$ real spacecraft charges only exist for $\theta = 0°$ or $\theta = 90°$. This is true because $\theta = 0°$ or $\theta = 90°$ are the only possible orientations for the unique charges. However in this case the charges on spacecraft aligned along the $\hat{\mathbf{o}}_\theta$ axis is not 0. The individual charges for such a formation are given by

$$\tilde{q}_1 = 2\sqrt{\frac{3}{7}}\sqrt{m\rho^3} \tag{42a}$$

$$\tilde{q}_2 = -4\sqrt{\frac{6}{7}}\sqrt{m\rho^3} \tag{42b}$$

$$\tilde{q}_3 = -2\sqrt{\frac{3}{7}}\sqrt{m\rho^3} \tag{42c}$$

$$\tilde{q}_4 = 4\sqrt{\frac{6}{7}}\sqrt{m\rho^3} \tag{42d}$$

Figures 7(a) and 7(b) show the plots of $\tilde{t}_i$ vs. θ for $\hat{\mathbf{o}}_r$-$\hat{\mathbf{o}}_h$ and $\hat{\mathbf{o}}_h$-$\hat{\mathbf{o}}_\theta$ plane respectively. Here the shaded area indicates the region for real spacecraft charges. The individual charges for $\hat{\mathbf{o}}_r$-$\hat{\mathbf{o}}_h$ plane can be calculated

13

by plugging in the value of t from (33) in Eq. (12a) to get $\tilde{q}_1$ in terms of ρ and θ, where $0 \leq \theta \leq 60$

$$\tilde{q}_1 = 2\sqrt{m\rho^3 \left(1 + 2\cos 2\theta\right)} \tag{43a}$$

$$\tilde{q}_2 = \sqrt{2m\rho^3 \left(1 + 2\cos 2\theta\right)} \tag{43b}$$

$$\tilde{q}_3 = -2\sqrt{m\rho^3 \left(1 + 2\cos 2\theta\right)} \tag{43c}$$

$$\tilde{q}_4 = -\sqrt{2m\rho^3 \left(1 + 2\cos 2\theta\right)} \tag{43d}$$

It is noted that for $\hat{\mathbf{o}}_h$-$\hat{\mathbf{o}}_\theta$ plane that the value of null-space scaling factor in Eq. (34a) does not yield real spacecraft charges for specific orientations of $\theta = 0°$ and $\theta = 90°$. The scaling factor from Eq. (34b) however allows the computation of real and spacecraft charge. The individual spacecraft charges are computed as

$$\tilde{q}_1 = \frac{1267}{1122}\sqrt{m\rho^3} \tag{44a}$$

$$\tilde{q}_2 = \frac{1409}{678}\sqrt{m\rho^3} \tag{44b}$$

$$\tilde{q}_3 = -\frac{1267}{1122}\sqrt{m\rho^3} \tag{44c}$$

$$\tilde{q}_4 = -\frac{1409}{678}\sqrt{m\rho^3} \tag{44d}$$

From figure 7(b) it is evident that a square formation in $\hat{\mathbf{o}}_h$-$\hat{\mathbf{o}}_\theta$ plane only exists for $\theta = 0°$ or $\theta = 90°$. The individual charges on spacecraft 2 and 4 are zero, as they lie along the $\hat{\mathbf{o}}_\theta$ plane. The square formation thus simplifies to a linear 2-craft formation in $\hat{\mathbf{o}}_h$ plane, solution to which has been discussed by Berryman and Schaub in reference 12. It is also noted from figure 7(b) that the value of null-space scaling factor in Eq. (30b) does not yield real spacecraft charges.

4-CRAFT STATIC COULOMB 3-D FORMATION SOLUTIONS

A tetrahedron is the one of the possible three-dimensional formations which satisfies the center of mass and the principal axes constraint for virtual Coulomb structures. An elegant property of tetrahedron is that the principal axes of tetrahedron can be aligned arbitrarily, and can be chosen in such a manner that the principal axes constraint is satisfied. Figure 8 shows the top and front view of a tetrahedron aligned along the $\hat{\mathbf{o}}_r$ axes. Spacecraft 1 is placed along the $\hat{\mathbf{o}}_r$ axes, the vertex of the tetrahedron. The remaining spacecraft form an equilateral triangle in the $\hat{\mathbf{o}}_h$-$\hat{\mathbf{o}}_\theta$ plane.

Charged Relative Equilibrium

There are several different attitude descriptions available to represent the orientation of the body frame with respect to the Hill frame. A sequence of Euler angles is used in the analysis presented here to describe the orientation of the body frame. A full 3-D rotation of a tetrahedron is quite complex for arbitrary orientations. Analysis of 2 angle rotation of tetrahedron for a range of the third angle provides a family of solutions for which a virtual tetrahedron exists. Let ψ, θ and ϕ represent the rotation angles about $\hat{\mathbf{o}}_r$, $\hat{\mathbf{o}}_\theta$ and $\hat{\mathbf{o}}_h$ axis respectively. The Hill frame position coordinates of the tetrahedron orientation after a sequential 3-2 Euler
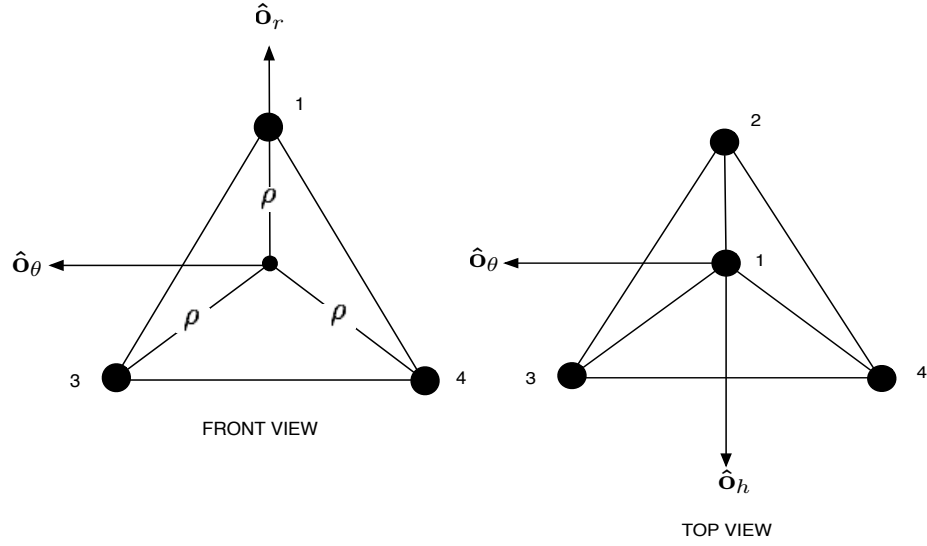
Figure 8 Parametrization of a Tetrahedron

angle rotation and $\psi = 0°$ is given by[22]

$$\rho_1 = \rho \begin{pmatrix} \cos\theta\cos\phi \\ \sin\phi\cos\theta \\ \sin\theta \end{pmatrix} \tag{45a}$$

$$\rho_2 = \frac{1}{3}\rho \begin{pmatrix} -cos\phi\left(\cos\theta + 2\sqrt{2}\sin\theta\right) \\ \sin\phi\left(-2\sqrt{2}\sin\theta - \cos\theta\right) \\ \sin\theta - 2\sqrt{2}\cos\theta \end{pmatrix} \tag{45b}$$

$$\rho_3 = \frac{1}{3}\rho \begin{pmatrix} -\cos\phi\left(\cos\theta - \sqrt{2}\sin\theta\right) - \sqrt{6}\sin\phi \\ \sqrt{6}\cos\phi - \sin\phi\left(\cos\theta - \sqrt{2}\sin\theta\right) \\ \sqrt{2}\cos\theta + \sin\theta\cos\phi \end{pmatrix} \tag{45c}$$

$$\rho_4 = \frac{1}{3}\rho \begin{pmatrix} -\cos\theta\ \cos\phi + \sqrt{2}\cos\phi\ \sin\theta + \sqrt{6}\sin\phi \\ -\sqrt{6}\cos\phi - \sin\phi\left(\cos\theta - \sqrt{2}\sin\theta\right) \\ \sqrt{2}\cos\theta + \sin\theta\cos\phi \end{pmatrix} \tag{45d}$$

For a three-dimensional formation, there are 12 charged spacecraft equations of motions, 4 each for the $\hat{\mathbf{o}}_r$, $\hat{\mathbf{o}}_h$ and $\hat{\mathbf{o}}_\theta$ axes. The number of these equations can be reduced by applying the center of mass conditions and principal axes constraints. For a three-dimensional formation there are 3 center of mass constraints and 3 principal axes constraints, reducing the number of equations to be solved to 6. Applying the center of mass and principal axes constraint and using Eqs. (5a)−(5c), the formation dynamics can be expressed in matrix form as

$$m \begin{bmatrix} 0 \\ 0 \\ 0 \\ z_1 \\ z_2 \\ -3x_1 \end{bmatrix} = \begin{bmatrix} \frac{y_1-y_2}{d_{12}^3} & \frac{y_1-y_3}{d_{13}^3} & \frac{y_1-y_4}{d_{14}^3} & 0 & 0 & 0 \\ \frac{y_2-y_1}{d_{12}^3} & 0 & 0 & \frac{y_2-y_3}{d_{23}^3} & \frac{y_2-y_4}{d_{24}^3} & 0 \\ 0 & \frac{y_3-y_1}{d_{13}^3} & 0 & \frac{y_3-y_2}{d_{23}^3} & 0 & \frac{y_3-y_4}{d_{34}^3} \\ \frac{z_1-z_2}{d_{12}^3} & \frac{z_1-z_3}{d_{13}^3} & \frac{z_1-z_4}{d_{14}^3} & 0 & 0 & 0 \\ \frac{z_2-z_1}{d_{12}^3} & 0 & 0 & \frac{z_2-z_3}{d_{23}^3} & \frac{z_2-z_4}{d_{24}^3} & 0 \\ \frac{x_1-x_2}{d_{12}^3} & \frac{x_1-x_3}{d_{13}^3} & \frac{x_1-x_4}{d_{14}^3} & 0 & 0 & 0 \end{bmatrix} \begin{bmatrix} \tilde{Q}_{12} \\ \tilde{Q}_{13} \\ \tilde{Q}_{14} \\ \tilde{Q}_{23} \\ \tilde{Q}_{24} \\ \tilde{Q}_{34} \end{bmatrix} \tag{46}$$

15

Equation (46) can be expressed in compact form using Eq. (7). The rank of matrix $[A]$ is 6, thus it is a full rank matrix and a unique solution to $\tilde{\mathbf{Q}} = [A]^{-1}\mathbf{x}$ is found. It is interesting to note that there is no null-space to exploit for a tetrahedron formation. There is only a unique set of charged products for the tetrahedron system expressed as

$$
\mathbf{Q}^* = \frac{1}{9}m\rho^3
\begin{bmatrix}
-4\sqrt{6}\left(3c^2\theta\ c^2\phi + \sqrt{2}c\theta\ s\theta\left(5 + 3c2\phi\right) - s^2\theta\right) \\
-\left(\sqrt{6} + 5\sqrt{6}c2\theta + 6\sqrt{6}c^2\theta\ c2\phi - 2\sqrt{3}s2\theta\left(5 + 3c2\phi\right) + 36c\theta\ s2\phi\right) \\
-\left(\sqrt{6} + 5\sqrt{6}c2\theta + 6\sqrt{6}c^2\theta\ c2\phi - 2\sqrt{3}s2\theta\left(5 + 3c2\phi\right) - 36c\theta\ s2\phi\right) \\
\sqrt{\frac{2}{3}}\left(-3 - 9c2\phi + 5c2\theta\left(5 + 3c2\phi\right) + \sqrt{2}s2\theta\left(5 + 3c2\phi\right) + 6\sqrt{6}c\theta\ s\phi + 24\sqrt{3}s\theta\ s2\phi\right) \\
\sqrt{\frac{2}{3}}\left(5c2\theta\left(5 + 3c2\phi\right) + \sqrt{2}s2\theta\left(5 + 3c2\phi\right) - 3s2\phi\left(1 + 3c2\theta + 2\sqrt{3}\left(\sqrt{2}c\theta + 4s\theta\right)\right)\right) \\
-\sqrt{\frac{2}{3}}\left(33 - 45c2\phi + c2\theta\left(5 + 3c2\phi\right) + 2\sqrt{2}s2\theta\left(5 + 3c2\phi\right)\right)
\end{bmatrix}
\tag{47}
$$

Angles θ and ϕ are used to represent the orientation of the tetrahedron in space. The third angle ψ is set to $0°$ to simplify these algebraic expressions. The charged product solution depends on the orientation of tetrahedron vertex.

Unique Individual Charges

From equation (9) it is seen that the charged products for a planar formation depend on the null-space of the system. The null-space can be exploited to find specific charged products which result in unique spacecraft charges. For a three-dimensional formation there is only a unique set of charged products, which depend on the orientation of the tetrahedron in the space. This differentiates the analysis of a three-dimensional formation to that of a planar formation. The analysis presented here determines the conditions for unique spacecraft charges for ranges of three-dimensional tetrahedron attitudes.

A tetrahedron can be broken into triangular loops as shown in figure 5, focused on spacecraft position 1 to compute the charge on spacecraft 1. The charge on spacecraft 1 can be computed as shown by Eqs. (12). For the planar formation the charged product solutions contains a 1-D null-space which yields infinity of potential $\tilde{Q}_{ij}$ solutions. By carefully choosing the value of the scaling parameter t it was shown that only one equality constraint from Eq. (12) is needed for unique spacecraft charges. With no null-space to exploit in a three-dimensional formation, the charge on spacecraft 1 $\tilde{q}_1$, should be unique to all the three loops in figure 5. Mathematically this condition is represented as

$$\tilde{Q}_{12}\tilde{Q}_{34} - \tilde{Q}_{14}\tilde{Q}_{23} = 0 \tag{48a}$$

$$\tilde{Q}_{13}\tilde{Q}_{24} - \tilde{Q}_{14}\tilde{Q}_{23} = 0 \tag{48b}$$

For a planar square formation if one equality constraint is satisfied, the other constraint is guaranteed to be satisfied as well. For a three-dimensional formation there are two equality constraints that need to be satisfied for unique spacecraft charges. The conditions on ϕ and θ must satisfy the equality constraints in (48a) and (48b) to obtain a unique spacecraft charge $\tilde{q}_1$. Using Eq. 47, the equality constraints in (48) are written as

$$\frac{64}{27}m^2\rho^6\left(3c^2\phi - 2\sqrt{3}c\phi\ s\phi\left(\sqrt{2}c\theta + s\theta\right) + 3s\theta\ s^2\phi\left(2\sqrt{2}c\theta - s\theta\right)\right) = 0 \tag{49a}$$

$$\frac{256}{9}m^2\rho^6 c\phi\ s\phi\left(\sqrt{2}c\theta + s\theta\right) = 0 \tag{49b}$$

From Eqs. (49a) and (49b), it is seen that regions where unique spacecraft charge exists are not intuitive. Figure 9(a) presents the contour plots for the equality constraints in Eqs. (49a) and (49b). Equation (49a) in figure 9(a) corresponds to constraint I and equation (49b) is represented by constraint II. The regions of unique charges are indicated by the points of intersection of two equality constraints. It is evident from figure 9(a) that unique charges on a tetrahedron exist for $\phi = 90°$ or $\phi = 270°$. Such an orientation corresponds to
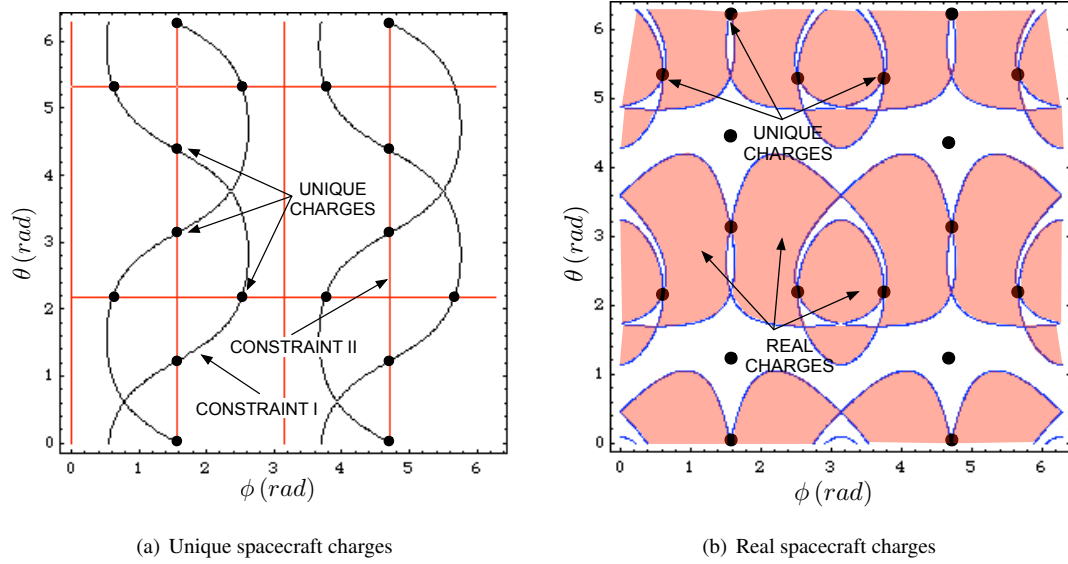
16

(a) Unique spacecraft charges

(b) Real spacecraft charges

Figure 9 Range of θ and ϕ for real and unique spacecraft charges for $\psi = 0°$

the vertex of the tetrahedron aligned with the $\hat{\mathbf{o}}_\theta$ direction, and the remaining spacecraft form an equilateral triangle in $\hat{\mathbf{o}}_r$-$\hat{\mathbf{o}}_h$ plane. The spacecraft 1 is aligned with $\hat{\mathbf{o}}_\theta$ axis for $\phi = 90°$ or $\phi = 270°$ only if $\psi = 0°$. Unique charges also do exist for other tetrahedron orientations, where the spacecraft is not aligned along $\hat{\mathbf{o}}_\theta$ axis.

Real Spacecraft Charges

As in case of a planar formation, finding the regions where the uniqueness conditions are satisfied is not sufficient for a virtual Coulomb structure. The individual charges on a spacecraft should also be real. The mathematical conditions for real charges used for planar formations in Eq. (35) are used for the tetrahedron formation. The inequality constraints in (35) imply that for each of the loops in the tetrahedron the individual spacecraft should be real. It was noted that for a 4-craft formation, if a unique charge $\tilde{q}_1$ exists, only one inequality constraint in Eq. (35) needs to be satisfied. Figure 9(b) shows the contour plot of the inequality constraint for real charges in Eq. (35a)

From figure 9(b) is it seen that individual charge $\tilde{q}_1$ on spacecraft 1 is real while the spacecraft is aligned with the $\hat{\mathbf{o}}_\theta$ axis. It is also seen that real charges are possible for orientations other than $\phi = 90°$ or $\phi = 270°$. Such orientations lie on the contours of the inequality constraint. This implies that the inequality constraint in equation (35a) is equal to 0 and one of the spacecraft charges is also 0. Thus the tetrahedron formation is reduced to a 3-craft equilateral triangle in $\hat{\mathbf{o}}_r$- $\hat{\mathbf{o}}_h$ plane. The analytic solution for the 3-craft formation is developed rigorously in reference 12 .

The analysis presented here assumes that $\psi = 0°$. Figure 10 shows the conditions for real and unique spacecraft charges on ϕ and θ, for different values of ψ. From the figure 10 it is seen that orientations for unique charges are only possible when the inequality constraint in Eq. (35a) is equal to 0. This implies one of the spacecraft charges is 0, and the formation simplifies to a 3-craft equilateral triangle formation.

The analysis of the three-dimensional tetrahedron formation assumed that the spacecraft have equal masses. It is however possible to have a tetrahedron formation oriented arbitrarily in space with variable mass. Analysis of the tetrahedron formation with variable mass needs to be addressed by future research work.
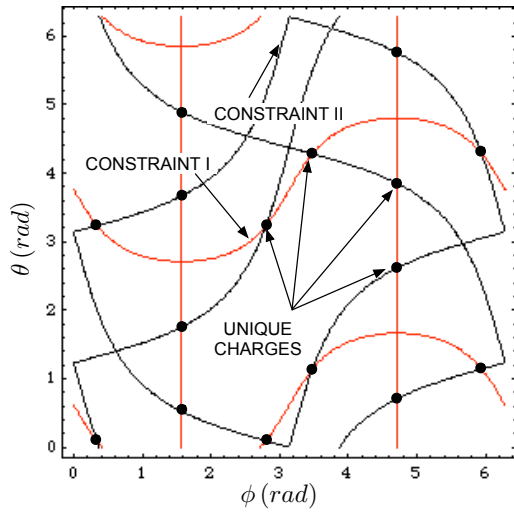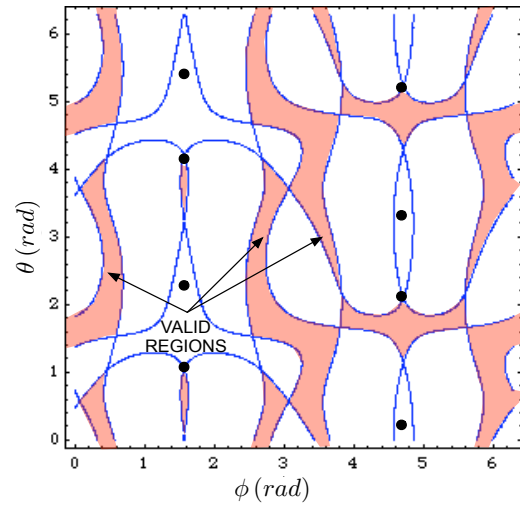
(a) Unique spacecraft charges for $\psi = 30°$
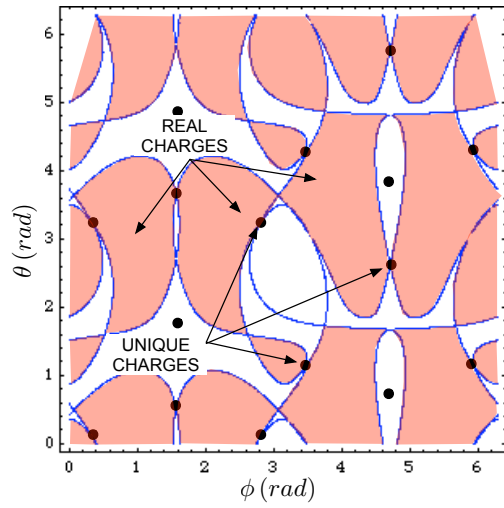
(b) Real spacecraft charges for $\psi = 30°$
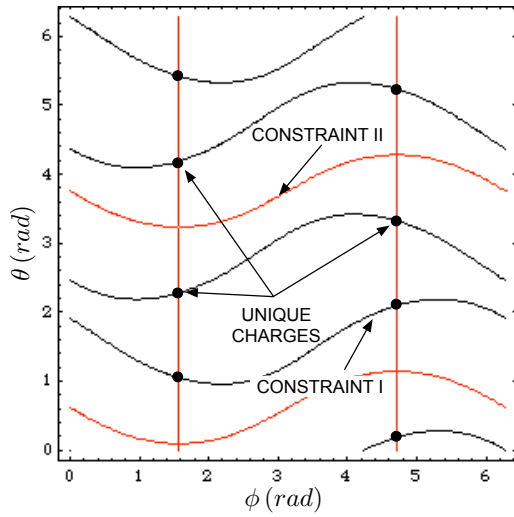
(c) Unique spacecraft charges for $\psi = 60°$

(d) Real spacecraft charges for $\psi = 60°$

Figure 10 Range of θ and ϕ for real and unique spacecraft charges

CONCLUSION

Coulomb thrusting offers an attractive solution as a controller in close proximity flying scenarios. Coulomb propulsion has no thruster exhaust and no damage occurs to near-by spacecraft. Coulomb thrusting also has the advantages of being essentially propellant-less and massless.

Analytical tools for determining the charge solution for static a 4-craft formation are discussed. Analytic solutions extend the work done on 2 and 3-craft formation and present an analysis on a 4-craft formation. For a 4-craft formation the issues of unique spacecraft charges and multiple real-charge inequality constraints arise for the first time.

Analytical charge solutions are investigated for a square Coulomb structure. The square formation is parameterized in terms of the radius ρ and orientation angle θ for any principal orbit plane choice. The range of angle θ where unique and real spacecraft charges exist are identified. Criteria are also presented for computing unique and real spacecraft charges. With a planar formation the charged products are a function of the null-space. By carefully choosing the null-space scaling parameter, the equality constraints for unique spacecraft charges is reduced. The solutions to the individual spacecraft charges is provided.

The paper also presents the analysis of a 3-D tetrahedron formation where all spacecraft have the same mass. The real and unique charge criteria are numerically investigated for arbitrary cluster orientations. The results indicated that only trivial solutions are possible with constant charges where one of the craft has zero charge and is located on the along-track axis.

ACKNOWLDEGEMENT

REFERENCES

[1] J. Bristow, D. Folta, and K. Hartman, "A Formation Flying Technology Vision," *AIAA 2000 Space Conference and Exposition*, Long Beach, CA, September 19-21 2000. Paper No. AIAA 2000-5194.

[2] M. Xin, S. Balakrishnan, and H. Pernicka, "Position and Attitude Control of Deep-Space Spacecraft Formation Flying via Virtual Structure and $\theta - D$ Technique," *AIAA Guidance Navigation and Control Conference and Exhibit*, San Francisco, CA, August 15-18 2005. Paper No. AIAA 2000-6090.

[3] P. Gurfil and N. Kasdin, "Dynamics and Control of Spacecraft Formation Flying in Three Body Trajectories," *AIAA Guidance Navigation and Control Conference and Exhibit*, Montreal, Canada, August 6-9 2001. Paper No. AIAA 2001-4026.

[4] J. Leitner, F. Bauer, D. Folta, M. Moreau, R. Carepenter, and J. How, "Formation Flight in Space: Distributed Spacecraft Systems Develop New GPS Capabilities," *GPS World*, Feb 2001.

[5] K. Torkar and et. al., "Spacecraft Potential Control aboard Equator-S as a Test for Cluster-II," *Annales Geophysicae*, Vol. 17, 1999, pp. 1582–1591.

[6] Schmidt and e. al, "Results from active spacecraft potential control on the Geotail spacecraft," *Journal of Geophysical Research*, Vol. 100, No. A9, 1995, pp. 253–259.

[7] T. Nakagawa, T. Ishii, K. Tsuruda, H. Hayakawa, and T. Mukai, "Net current density of photoelectrons emitted from the surface of the GEOTAIL spacecraft," *Earth Space and Planets*, Vol. 52, 2000, pp. 283–292.

[8] C. P. Escoubet, M. Fehringer, and M. Goldstein, "The Cluster Mission," *Annales Geophysicae*, Vol. 19, No. 10/12, 2001, pp. 1197–1200.

[9] K. Torkar, W. Riedler, C. P. Escoubet, and e. al, "Active Spacecraft Potential Control for Cluster – Implementation and First Results," *Annales Geophysicae*, Vol. 19, No. 10/12, 2001, pp. 1289–1302.

[10] L. King, G. Parker, and S. Deshmukh, "Spacecraft Formation Flying using Inter-Vehicle Coulomb Forces," tech. rep., NASA/NIAC, January 2002.

[11] L. King, G. Parker, and S. Deshmukh, "Study of Interspacecraft Coulomb Forces and Implication for Formation Flying," *AIAA Journal of Propulsion and Power*, Vol. 19, No. 3, May-June 2003.

[12] J. Berryman and H. Schaub, "Analytical Charge Analysis for 2- and 3-Craft Coulomb Formations," *AAS/AIAA Astrodynamics Specialist Conference*, Lake Tahoe, CA, August 7–11 2005. Paper No. AAS 05–278.

[13] A. Natarajan, H. Schaub, and G. G. Parker, "Reconfiguration of a 2-Craft Coulomb Tether," *AAS Space Flight Mechanics Meeting*, Tampa, FL, Jan. 22–26 2006. Paper No. AAS-06-229.

[14] H. Schaub, C. Hall, and J. Berryman, "Necessary Conditions for Circularly-Restricted Static Coulomb Formations," *AAS Malcolm D. Shuster Astronautics Symposium*, Buffalo, NY, June. 12–15 2005. Paper No. AAS 05–472.

[15] A. Natarajan and H. Schaub, "Linear Dynamics and Stability Analysis of a Coulomb Tether Formation," *AIAA Journal of Guidance, Control, and Dynamics*, Vol. 29, July–Aug. 2006, pp. 831–839.

[16] A. Natarajan and H. Schaub, "Hybrid Conrol of Orbit Normal and Along-Track 2-Craft Coulomb Tethers," *AAS Space Flight Mechanics Meeting*, Sedona, AZ, Jan. 28–Feb. 1 2007. Paper AAS 07–193.

[17] H. Schaub and M. Kim, "Orbit Element Difference Constraints for Coulomb Satellite Formations," *AIAA/AAS Astrodynamics Specialist Conference*, Providence, Rhode Island, Aug. 2004. Paper No. AIAA 04-5213.

[18] S. Wang and H. Schaub, "Spacecraft Collision Avoidance Using Coulomb Forces With Separation Distance Feedback," *AAS Space Flight Mechanics Meeting*, Sedona, AZ, Jan. 28–Feb. 1 2007. Paper AAS 07–112.

[19] L.Pettazzi, D.Izzo, and S.Theil, "Swarm Navigation and Reconfiguration using Electrostatic Forces," *7th International Conference on Dynamics and Control of Systems and Structures in Space*, Greenwich, London, England, July 19–20 2006.

[20] D. Izzo and L. Pettazzi, "Self-assembly of large structures in Space using inter-satellite Coulomb forces," *56th International Astronautical Congress*, Fukuoka, Japan, Oct. 17-21 2005.

[21] S. Wang and H. Schaub, "One-Dimensional 3-Craft Coulomb Structure Control," *7th International Conference on Dynamics and Control of Systems and Structures in Space*, Greenwich, London, England, July 19–20 2006, pp. 269–278.

[22] H. Vasavada, "Four-Craft Virtual Coulomb Structure Analysis for 1 to 3 Dimensional Geometries," Master's thesis, Virginia Tech, 2007.